Global PROTOMAP Profiling to Search for Biomarkers of Early-Recurrent Hepatocellular Carcinoma

ARTICLE *in* JOURNAL OF PROTEOME RESEARCH · JUNE 2014

Impact Factor: 4.25 · DOI: 10.1021/pr500262p · Source: PubMed

12 AUTHORS, INCLUDING:

Hidenori Ojima
Japan Research Institute
78 PUBLICATIONS **1,805** CITATIONS
SEE PROFILE

Daisuke Kubota
National Cancer Center, Japan
36 PUBLICATIONS **171** CITATIONS
SEE PROFILE

Tadashi Kondo
National Cancer Center, Japan
149 PUBLICATIONS **2,559** CITATIONS
SEE PROFILE

Journal of proteome research

Article

pubs.acs.org/jpr

Global PROTOMAP Profiling to Search for Biomarkers of Early-Recurrent Hepatocellular Carcinoma

Masato Taoka,[†] Noriaki Morofuji,[▽,‡] Yoshio Yamauchi,[†] Hidenori Ojima,[○,§] Daisuke Kubota,[‡] Goro Terukina,[†] Yuko Nobe,[†] Hiroshi Nakayama,[∥] Nobuhiro Takahashi,[⊥] Tomoo Kosuge,[#] Toshiaki Isobe,*[,†] and Tadashi Kondo*[,‡]

[†]Department of Chemistry, Graduate School of Sciences and Engineering, Tokyo Metropolitan University, Minamiosawa 1-1, Hachioji-shi, Tokyo 192-0397, Japan

[‡]Division of Pharmacoproteomics and [§]Division of Molecular Pathology, National Cancer Center Research Institute, 5-1-1 Tsukiji, Chuo-ku, Tokyo 104-0045, Japan

[∥]Biomolecular Characterization Team, RIKEN Advanced Science Institute, 2-1, Hirosawa, Wako, Saitama 351-0198, Japan

[⊥]Department of Biotechnology, United Graduate School of Agriculture, Tokyo University of Agriculture and Technology, Saiwai-cho 3-5-8, Fuchu-shi, Tokyo 183-8509, Japan

[#]Hepatobiliary and Pancreatic Surgery Division, National Cancer Center Hospital, 5-1-1 Tsukiji, Chuo-ku, Tokyo 104-0045, Japan

Supporting Information

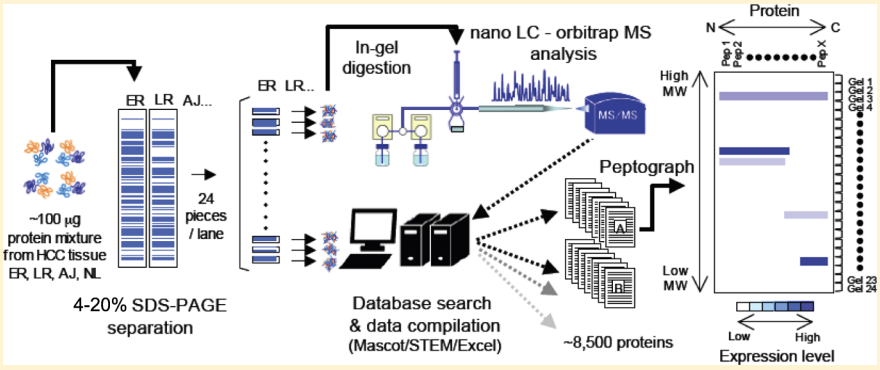

ABSTRACT: This study used global protein expression profiling to search for biomarkers to predict early recurrent hepatocellular carcinoma (HCC). HCC tissues surgically resected from patients with or without recurrence within 2 years (early recurrent) after surgery were compared with adjacent nontumor tissue and with normal liver tissue. We used the PROTOMAP strategy for comparative profiling, which integrates denaturing polyacrylamide gel electrophoresis migratory rates and high-resolution, semiquantitative mass-spectrometry-based identification of in-gel-digested tryptic peptides. PROTOMAP allows examination of global changes in the size, topography, and abundance of proteins in complex tissue samples. This approach identified 8438 unique proteins from 45 708 nonredundant peptides and generated a proteome-wide map of changes in expression and proteolytic events potentially induced by intrinsic apoptotic/necrotic pathways. In the early recurrent HCC tissue, 87 proteins were differentially expressed (≥20-fold) relative to the other tissues, 46 of which were up-regulated or specifically proteolyzed and 41 of which were down-regulated. This data set consisted of proteins that fell into various functional categories, including signal transduction and cell organization and, notably, the major catalytic pathways responsible for liver function, such as the urea cycle and detoxification metabolism. We found that aberrant proteolysis appeared to occur frequently during recurrence of HCC in several key signal transducers, including STAT1 and δ-catenin. Further investigation of these proteins will facilitate the development of novel clinical applications.

KEYWORDS: *hepatocellular carcinoma, biomarker, PROTOMAP, proteomics, mass spectrometry*

INTRODUCTION

Hepatocellular carcinoma (HCC) is one of the most common and aggressive malignancies and is the third leading cause of cancer deaths worldwide.[1] Although early diagnosis and subsequent treatments have considerably improved overall survival, long-term survival rates remain low because of a high

Special Issue: Proteomics of Human Diseases: Pathogenesis, Diagnosis, Prognosis, and Treatment

Received: March 14, 2014

   dx.doi.org/10.1021/pr500262p | *J. Proteome Res.* XXXX, XXX, XXX−XXX

incidence of recurrence and metastasis.[2−7] Several pathological and clinical parameters are used to assess the malignant features of HCC and predict the prognosis after treatment, including histological differentiation, size of tumor, vascular invasion, and liver function.[8] However, a substantial subset of HCC tumors that are classified as low risk still progress to metastasis after treatment. Further investigation of the underlying mechanisms that determine malignant potential in HCC is necessary to optimize therapeutic strategies for individual patients.

Global gene and protein expression studies of primary tumor tissues have been a central tool in the development of prognostic biomarkers for HCC. Iizuka et al. examined mRNA expression in tissues of patients with different prognoses and identified a set of 12 genes associated with recurrence.[9] Ye et al. also identified a gene expression signature for the metastatic potential of HCC through global gene expression analysis.[10] These studies also provide insight into the malignant features of HCC.[11]

Using a 2-D difference gel-electrophoresis-based proteomics approach, we identified adenomatous polyposis coli (APC)-binding protein EB1 as a prognostic biomarker for HCC.[12] Similar studies identified calpain small subunit 1,[13] mortalin,[14] and talin-1[15] as prognostic biomarker candidates from clinical samples. Although these studies show the utility of proteomics in identifying biomarkers, posttranslational modifications of proteins were not considered in these studies.

Tissue homeostasis is severely disrupted in HCC by excessive proliferation of apoptosis-resistant cancer cells, which can alter the degree of caspase-related proteolysis.[16,17] This proteolysis is a key regulatory mechanism of normal physiological processes that promote development,[18,19] blood coagulation,[20] and cell death,[21] and proteolytic dysfunction is associated with many pathological events such as infectious disease[22] and cancer.[23] To date, ∼100 specific proteolysis-related hereditary diseases have been recognized, and for many of these diseases the levels of aberrant proteolytic fragments correlate with the severity of symptoms.[24] In fact, several proteolytic fragments, such as the ectodomain fragment derived from epithelial growth factor receptor-2[25] and the soluble fragment from cytokeratin 19,[26] have been found in the biological fluids of cancer patients and are considered potential cancer biomarkers. Thus, analysis of proteolytic events may be particularly useful in searching for prognostic biomarkers for HCC.

Recently, a novel proteomics approach, referred to as the Protein Topography and Migration Analysis Platform (PROTOMAP), was established to examine proteolytic events.[27] In this method, a sample mixture is first separated by conventional sodium dodecyl sulfate-polyacrylamide gel electrophoresis (SDS-PAGE), the gel lanes are cut into bands at fixed intervals, the cut bands are digested with trypsin, and the released peptides are analyzed by reversed-phase liquid chromatography−tandem mass spectrometry (LC−MS/MS). The resulting proteomic data are integrated into peptographs, which plot sequence coverage for a given protein in the horizontal dimension versus SDS-PAGE migration in the vertical dimension; thus, proteins that undergo proteolytic cleavage are identified by shifts in migration from higher to lower molecular weight species. This method has been used to generate a proteome-wide map of proteolytic events induced by the intrinsic apoptotic pathway and has uncovered many previously undocumented caspase substrates.[27] Similarly, the PROTOMAP method has been used to examine differences in metastatic potential in liver cancer cell lines, and these studies revealed that calpain-2 and related proteins are associated with liver cancer metastasis.[28]

Here we applied the PROTOMAP strategy for global comparative profiling of HCC to identify novel biomarkers that could be used to evaluate malignancy and predict recurrence. We performed large-scale comparative proteomic profiling of HCC tissues surgically resected from patients with or without recurrence within 2 years after surgery-early recurrent (ER)- and late-recurrent (LR)-HCC tissues, respectively, as well as of adjacent nontumor tissue and normal liver tissue. To improve the accuracy of the quantitative index, we modified the original procedure by replacing simple spectral counts with the exponentially modified protein abundance index (emPAI).[29] Our analysis generated a large data set of HCC differentiation- and malignancy-associated proteins and proteolytic products that may serve as useful prognostic and therapeutic targets to prevent HCC recurrence.

MATERIALS AND METHODS

Chemicals and Antibodies

All chemicals used in this study were obtained from Wako Pure Chemical Industries (Osaka, Japan), unless otherwise indicated. Antibodies against the Signal Transducers and Activators of Transcription family protein 1 (STAT1) C-terminal sequences (#9175), δ-catenin (#610133), and actin (#A5060) were purchased from Cell Signaling Technology (Danvers, MA), BD Biosciences (San Jose, CA), and Sigma-Aldrich (St. Louis, MO), respectively.

Patients and Tissue Samples

All tissues used in this study were obtained from patients at the National Cancer Center Hospital, Tokyo, Japan. Clinical and pathological information for these patients is summarized in Supplementary Table 1 in the Supporting Information. The diagnosis of liver cancer was made by ultrasonography and dynamic computed tomography or magnetic resonance imaging, and the diagnosis of HCC was confirmed by pathological examination of the resected tissues after surgery. From the patients with HCC, tissues were obtained at a time of initial surgery. The HCC patients had recurrence within 2 years after the surgery (ER-HCC) or did not have recurrence within the same term (LR-HCC). The nontumor tissues adjacent to the tumor (AJ), all but two of which had developed hepatitis or cirrhosis, were also collected at the time of surgery. These tissues did not have micro metastasis, as examined by microscopic inspection. The normal liver tissues (NL) were obtained from liver of the colorectal cancer patients who had recurrence in liver. While all patients with early recurrence exhibited portal vein invasion, the patients in the LR-HCC group did not have it. All but two patients with early recurrence had recurrent tumor(s) in remnant liver (Supplemental Table 1 in the Supporting Information). Although we could not exclude the possibility that the early recurrence might include possible incomplete resection, we included all such cases in this study. The virus infection was observed in 16 cases of 20 HCC patients who provided tumor tissues in this study (Supplemental Table 1 in the Supporting Information). All tissues were immediately frozen at −80 °C after surgery. The Ethics Committee of National Cancer Center approved this study, and all patients participating in this study provided written, informed consent. We performed all experiments under the strict risk management to prevent virus infection according to the regulations of National Cancer Center Research Institute.

dx.doi.org/10.1021/pr500262p | J. Proteome Res. XXXX, XXX, XXX−XXX

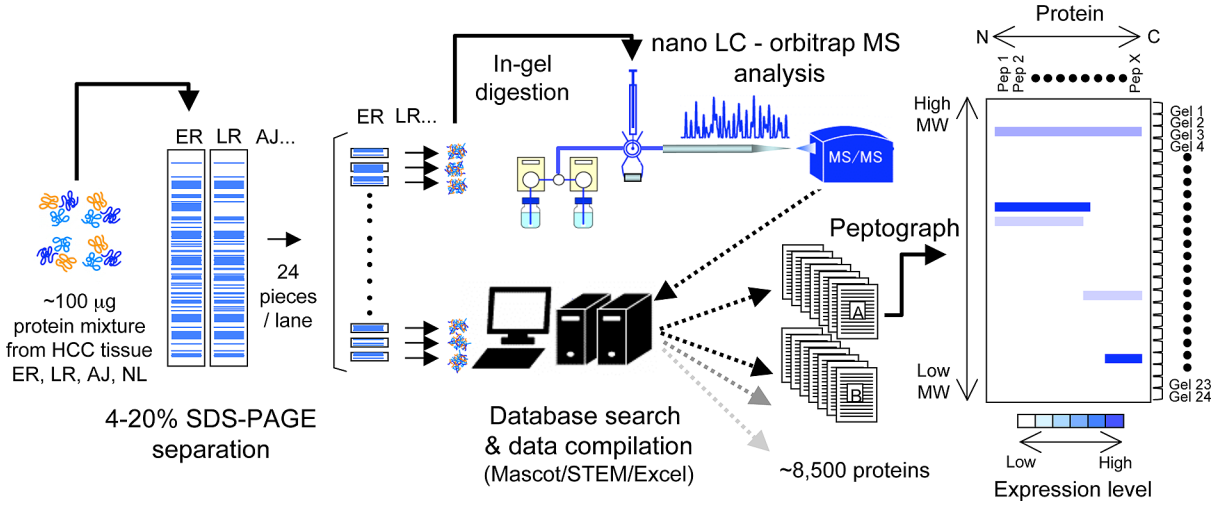

Figure 1. Schematic illustration of PROTOMAP strategy used in this study. Details are given in the text.

Sample Preparation, SDS-PAGE, LC–MS/MS Analysis, and Peptograph Assembly

The experimental procedure used in this study is illustrated in Figure 1. Tissue samples (100 μg protein) were separated by 4–20% SDS-PAGE, and the gel lanes were cut into 24 pieces at fixed intervals (0.5 cm bands). Each gel piece was incubated with 0.25 μg trypsin in 20 μL of Tris-HCl (pH 8.8) overnight at 37 °C,[30] and the resulting peptide mixture was analyzed on a direct nanoflow LC–MS/MS system equipped with an Orbi-Trap mass spectrometer (Orbi-Trap XL, Thermo Scientific, Boston, MA), as described.[31] In brief, peptides were separated on a reversed-phase tip column (150 μm [i.d.] × 70 mm, Mightysil-C18, 3 μm particle) using a linear gradient starting at 100% A [A: 0.1% (v/v) formic acid in water] at 100 nL/min. The mobile phase was 0–35% B [B: 0.1% (v/v) formic acid in acetonitrile] for 70 min. The column was subsequently washed with 70% B for 10 min and re-equilibrated with 100% A for the next analysis. Full MS scans were acquired with a resolution of 30 000 at a mass-to-charge ratio of 400. The 10 most intense ions were fragmented in a data-dependent mode by collision-induced dissociation with normalized collision energy of 35, activation q of 0.25, and activation time of 10 ms and one microscan. The fragments were then analyzed in ion trap MS using the following conditions: spray voltage, 2.0 kV; ion transfer tube temperature, 200 °C; ion selection threshold, 10 000 counts; maximum ion accumulation times, 500 ms for full scans; and dynamic exclusion duration, 60 s (10 ppm window; maximum number of excluded peaks, 500). The MS/MS data were converted to the mascot generic format with the Proteome Discoverer software (Thermo Scientific, ver. 1.1). The files were processed with the MASCOT algorithm (version 2.2.1., Matrix Science, London, United Kingdom) to assign peptides using the Swiss-Prot sequence database (release 2011; 20 236 sequences, human) under the search parameters as described.[31] Peptide identifications were based on the MASCOT definitions, except that we used stricter protein assignment criteria than the standard defaults.[32] In brief, we set the variable modification parameters for acetylation (protein N-terminus) and oxidation (Met). The maximum missed cleavage was set at 1 with a peptide mass tolerance of ±15 ppm. Peptide charges from +2 to +4 states and MS/MS tolerances of ±0.8 Da were allowed. We selected the candidate peptides with probability-based Mowse scores (total score) that exceeded their threshold, indicating a significant homology ($p < 0.05$), and referred to them as "hits". The criteria were based on the vendor's definitions (Matrix Science). Furthermore, we set more strict criteria for protein assignment: (1) any peptide candidate with an MS/MS signal number of <2 was eliminated from the "hit" candidates, regardless of the match score (total score minus threshold); (2) proteins with match scores exceeding 10 ($p < 0.005$) were referred to as "identified"; and (3) if the protein was identified with a single peptide candidate having a match score lower than 10, the original MS/MS spectrum was carefully inspected to confirm that the assignment was based on three or more y- or b-series ions. All results of peptide searches were extracted from the Mascot DAT files using the STEM[33] software, expressed as tab-delaminated text files, and pooled in a spreadsheet of Microsoft Excel (Excel 2010, Microsoft, Albuquerque, NM). The identified peptides were then grouped into each particular protein that the peptide can be produced and sorted according to its sequence using the commands defined by the vendor.

The resulting data were integrated into heat map "peptographs", as described by Dix et al.,[27] except that we used the emPAI parameters[29] instead of simple spectral counts to estimate semiquantitative differences in the identified peptides. Specifically, in the peptographs, identified peptides for a given protein were plotted in the vertical dimension (N to C terminus, top to bottom), and SDS-PAGE migration of the protein was plotted in the horizontal dimension (high to low molecular weight, left to right). The semiquantitative differences in proteins estimated by the emPAI are represented in the peptographs by the depth of blue color (light to dark, low to high abundance) using a spreadsheet program (Excel 2010).

To evaluate the levels of specific proteins in the ER-HCC, LR-HCC, AJ, and NL tissues, we estimated a sum of emPAI parameters (Σ_{emPAI}) from the corresponding peptographs. If the Σ_{emPAI} value for a given protein in the ER-HCC tissue was >20-fold higher than the values in the LR-HCC, AJ, and NL tissues, we tentatively designated the protein as up-regulated. Conversely, if the Σ_{emPAI} value for a protein in the ER-HCC tissue was >20-fold lower than the values in any other tissues, we tentatively designated the protein as down-regulated.

Western Blotting

Proteins (15 μg) in crude tissue extracts were separated by SDS-PAGE on 4–20% gradient gels (Criterion TGX, Bio-Rad,

dx.doi.org/10.1021/pr500262p | J. Proteome Res. XXXX, XXX, XXX–XXX

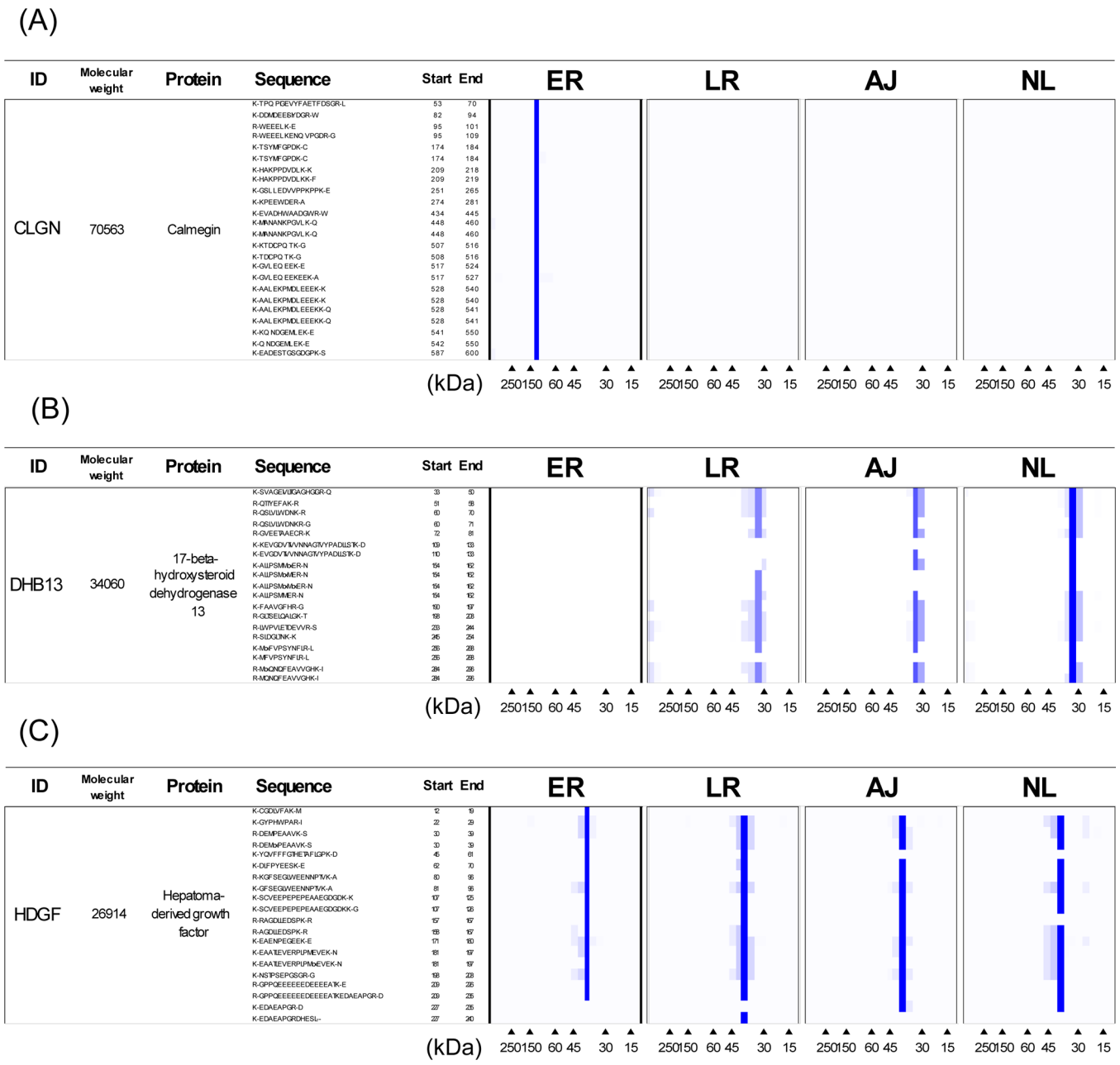

Figure 2. Representative peptographs of (A) calmegin, a protein that was up-regulated in ER-HCC tissue, (B) 17-β-hydroxysteroid dehydrogenase 13, a protein that was down-regulated in ER-HCC tissue, and (C) hepatoma-derived growth factor, a protein that did not appear to be affected by tumorigenesis. The vertical dimension shows the sequence of the identified protein from the N to the C terminus (top to bottom), and the horizontal dimension shows the SDS-PAGE–determined molecular weights (high to low, left to right, indicated at the bottom). The semiquantitative differences in protein and degradation product abundance, estimated by the emPAI, are reflected in the depth of the blue color (dark to light, high to low).

Hercules, CA) and transferred electrophoretically to polyvinylidene difluoride membranes (Trans-Blot Turbo, Bio-Rad). The membranes were blocked with StartingBlock blocking buffer (Thermo Scientific, Bremen, Germany) for 1 h at room temperature and then incubated with the appropriate antibodies overnight at 4 °C. The membranes were washed three times with StartingBlock blocking buffer for 10 min, incubated with horseradish peroxidase-conjugated secondary antibodies (1:10 000 dilution; GE Healthcare Bio-Sciences (Uppsala, Sweden) for 1 h at room temperature, washed three times with StartingBlock blocking buffer for 1 h, and visualized by enhanced chemiluminescence on Hyperfilm (GE Healthcare).

RESULTS AND DISCUSSION

Generation of Peptographs of HCC and Surrounding Liver Tissues

Proteins in crude extracts of the ER- and the LR-HCC tissues as well as the AJ and NL controls were separated in parallel lanes by SDS-PAGE. Samples 18 (NL), 24 (AJ), 37 (LR), and 16 (ER) were examined (Supplemental Table 1 in the Supporting Information). Immediately after electrophoresis, each sample lane was cut into 24 gel pieces at fixed intervals, and the proteins in each piece were in-gel digested with trypsin and analyzed by nanoflow reversed-phase LC–MS/MS for

dx.doi.org/10.1021/pr500262p | J. Proteome Res. XXXX, XXX, XXX–XXX

Table 1. Proteins Up-Regulated in the ER-HCC Tissue

UniProt ID	protein	molecular mass (kDa)	ΣemPAI maximum	degradation detected	oxido-reductase[a]	liver-specific expression[b]	phospho-protein[a]	previously reported HCC marker	ref
STAT1_HUMAN	signal transducer and activator of transcription 1-alpha/beta	87990	294.4	+	−	−	+	−	
GAGB1_HUMAN	G antigen family B member 1	16354	77.5	+	−	−	+	−	
CLGN_HUMAN	calmegin	70663	75.3	−	−	−	+	−	
LASP1_HUMAN	LIM and SH3 domain protein 1	30195	683	+	_	_	+	_	
SFPQ_HUMAN	splicing factor, proline- and glutamine-rich	76244	465	+	−	−	+	−	
PDIA2_HUMAN	protein disulfide-isomerase A2	58596	40.1	−	−	−	−	−	
CTND1_HUMAN	catenin delta-1	108814	39.9	+	−	−	+	−	
CKAP4_HUMAN	cytoskeleton-associated protein 4	66125	37.6	+	_	_	+	−	
ACOX3_HUMAN	peroxisomal acyl-coenzyme A oxidase 3	78503	36.2	+	+	−	+	−	
CLIP1_HUMAN	CAP-Gly domain-containing linker protein 1	163070	34.5	−	−	−	+	−	
ILEU_HUMAN	leukocyte elastase inhibitor	42857	34.4	+	−	−	+	−	
GALK1_HUMAN	galactokinase	42814	33.5	+	−	−	−	−	
FINC_HUMAN	fibronectin	266935	32.3	−	−	−	+	+	47−49
SYVC_HUMAN	valyl-tRNA synthetase	141950	31 3	+	_	_	+	_	
SYAC_HUMAN	alanyl-tRNA synthetase, cytoplasmic	107667	28.4	+	_	_	+	−	
PABP1_HUMAN	polyadenylate-binding protein 1	70910	28.3	+	_	−	+	−	
LGAT1_HUMAN	acyl-CoA: lysophosphatidylglycerol acyltransferase 1	43345	27.4	−	−	−	−	−	
ACACA_HUMAN	acetyl-CoA carboxylase 1	267516	26.0	+	−	−	+	−	
LPP1_HUMAN	lipid phosphate phosphohydrolase 1	32633	25.5	−	−	+	−	−	
HSPB1_HUMAN	heat shock protein beta-1	22840	25.5	+	−	±	+	+	50−52
SERPH_HUMAN	serpin H1	46553	24.7	+	_	_	_	_	
DHSA_HUMAN	succinate dehydrogenase flavoprotein subunit	73924	24.6	+	+	_	+	−	
AKA12_HUMAN	A-kinase anchor protein 12	192077	24.2	+	_	_	+	_	
DYHC1_HUMAN	cytoplasmic dynein 1 heavy chain 1	536482	24.0	+	_	_	+	−	
1C12_HUMAN	HLA class l histocompatibility antigen, Cw-12 alpha chain	41428	24.0	+	_	_	+	−	
SYWC_HUMAN	tryptophanyl-tRNA synthetase, cytoplasmic	53558	23.8	+	_	_	+	−	
TBB2A_HUMAN	tubulin beta-2A chain	50372	23.3	+	−	−	+	−	
1A01_HUMAN	HLA class I histocompatibility antigen, A-1 alpha chain	41175	23.1	+	−	−	+	−	
CLIP2_HUMAN	CAP-Gly domain-containing linker protein 2	116335	23.0	+	−	−	+	_	
UBA7_HUMAN	ubiquitin-like modifier-activating enzyme 7	112832	22.7	+	−	±	_	_	
1A36_HUMAN	HLA class I histocompatibility antigen, A-36 alpha chain	41263	22.5	+	−	−	+	−	
TIF1B_HUMAN	transcription intermediary factor 1-beta	90696	22.2	+	−	±	+	−	
TCPB_HUMAN	T-complex protein 1 subunit beta	57878	22.0	+	−	−	−	+	53
HNRPK_HUMAN	heterogeneous nuclear ribonucleoprotein K	51300	21 7	+	_	−	+	−	
HIP1R_HUMAN	huntingtin-interacting protein 1 -related protein	120167	21 6	−	_	+	+	−	
1C14_HUMAN	HLA class 1 histocompatibility antigen, Cw-14 alpha chain	41380	21.5	+	_	−	+	−	
AP3B1_HUMAN	AP-3 complex subunit beta-1	121955	21.3	+	−	±	+	−	
CO2_HUMAN	complement C2	84919	21.1	−	−	−	−	−	
1C04_HUMAN	HLA class I histocompatibility antigen, Cw-4 alpha chain	41467	21.0	+	−	−	+	−	
VIGLN_HUMAN	vigilin	142150	20.9	+	−	_	+	_	
ADRO_HUMAN	NADPH:adrenodoxin oxidoreductase, mitochondrial	54371	20.9	+	+	_	_	_	

dx.doi.org/10.1021/pr500262p | J. Proteome Res. XXXX, XXX, XXX−XXX

Table 1. continued

UniProt ID	protein	molecular mass (kDa)	ΣemPAI maximum	degradation detected	oxido-reductase[a]	liver-specific expression[b]	phospho-protein[a]	previously reported HCC marker	ref
DX39B_HUMAN	spliceosome RNA helicase DDX39B	49528	20.6	+	–	–	–	–	
FKBP4_HUMAN	peptidyl-prolyl cis–trans isomerase FKBP4	52127	20.4	+	–	±	+	–	
ACSL4_HUMAN	long-chain-fatty-acid-CoA ligase 4	80486	20.3	+	–	–	–	+	54
SYQ_HUMAN	glutaminyl-tRNA synthetase	88879	20.2	+	–	–	+	–	
HYOU1_HUMAN	hypoxia up-regulated protein 1	111550	20.1	+	–	++	–	–	

[a]According to the UniProt database. [b]±, ubiquitous; +, moderately specific; ++, highly specific.

protein identification. Duplicate analysis of each sample set identified 6218, 5857, 6010, and 5495 unique proteins based on 31 747, 31 419, 29 471, and 25 982 nonredundant peptides in the ER-HCC, LR-HCC, AJ, and NL tissues, respectively (Supplementary Table 2–5 in the Supporting Information). Overall, 8438 unique proteins were identified in the HCC and surrounding liver tissues (Supplementary Table 6 in the Supporting Information), which fell into a wide range of molecular weights (ranging from 5 kDa for thymosin β-10 to 3850 kDa for titin), subcellular compartments, and biological processes (Supplementary Figure 1A–C in the Supporting Information). The data sets obtained from the tissue samples were then integrated into peptographs (Supplementary Table 6 in the Supporting Information), which display differences in protein profiles between tissues on a proteome-wide scale. The peptographs also allowed visualization of potential proteolytic events that might be induced by the intrinsic apoptotic or necrotic proteolytic pathways during tumorigenesis. Representative portions of some of the peptographs are shown in Figure 2A–C.

Proteins Characteristic of ER-HCC Tissue

To search for ER-HCC–specific marker candidates, we focused on the proteins or proteolytic fragments that were specifically up- or down-regulated in the ER-HCC tissue. We selected 46 proteins that were up-regulated in ER-HCC tissue and 41 that were down-regulated (Tables 1 and 2). According to DAVID (Database for Annotation, Visualization and Integrated Discovery; http://david.niaid.nih.gov) categorization, the up-regulated proteins were involved in various cellular processes, including signal transduction, tRNA aminoacylation, protease inhibition, protein folding, and cell organization. Interestingly, we found that most of these up-regulated proteins (38/46) were specifically proteolyzed in the ER-HCC tissue (Table 1), and, according to the DAVID analysis, many of those (30/38) are potential phosphoproteins. Although the biological significance of this finding is unclear, it may be that atypical phosphoprotein degradation occurs in ER-HCC tissues, which inhibits normal phosphorylation-mediated signal transduction. As discussed in greater detail later, the peptograph analysis clearly detected proteolysis of two key phosphorylation-induced apoptotic signal transducers, STAT1 and δ-catenin, only in the ER-HCC tissue (Figure 3A,B).

We also found that several functional categories were overrepresented in the 41 down-regulated proteins detected in the ER-HCC tissue. First, 16 of the 41 proteins were oxidoreductases, consistent with previous reports that oxidoreductases are repressed in human, animal, and cultured hepatomas[34−39] (Table 2). For instance, levels of alcohol dehydrogenase 4 (ADH4) in HCC tissue are closely and negatively correlated with the pathology grade of the tumor and with levels of the tumor marker serum α-fetoprotein.[40] Likewise, HCC patients with low ADH4 expression levels have much lower overall survival rates than do those with high expression levels. In this study, we found that ADH4 levels were reduced in ER-HCC tissues and that the levels were substantially and negatively correlated with recurrence in patients with HCC. It should also be noted that 10 of the ER-HCC-specific proteins that we identified are previously known tumor marker candidates (Tables 1 and 2).

The down-regulated protein subset also contained many proteins that are liver-specific or are highly expressed in the liver and are involved in the catalytic pathways responsible for major liver functions, such as the urea cycle and detoxification metabolism. Of the 22 down-regulated proteins with available tissue distribution information in the UniProt database, 16 were categorized as specifically expressed or highly expressed in the liver, whereas only 3 of the 17 up-regulated proteins with tissue distribution information were categorized as liver-specific, suggesting that ER-HCC tissue contains many undifferentiated or dedifferentiated cells. Stem-like cells with their progeny have been observed in tumor tissues, and these cells have aberrant differentiation capacity or promote metastatic spread of tumor cells.[18,41] Taken together with our results, this suggests that stem-like cells that remain after surgery might cause early recurrence of HCC.

The results previously described indicate that the PROTOMAP strategy will be useful in the discovery of proteins associated with the malignant potential of HCC cells. Early recurrence of HCC was accompanied by portal vein invasion (Supplemental Table 1 in the Supporting Information), suggesting that aberrant regulation of the identified proteins may increase the invasiveness of tumor cells. Thus, these proteins are potential biomarkers for early recurrence and potential therapeutic targets.

Proteolytic Fragments of STAT1 and δ-Catenin

Our peptograph analysis detected proteolytic fragments of many proteins in HCC and surrounding liver tissues, particularly in ER-HCC tissue (Table 1). Although it is possible that some of these fragments were generated during storage or handling of tissue samples, this proteolysis might suggest that intrinsic apoptotic or necrotic proteolytic events contribute to tumorigenesis or recurrence of HCC. Of particular interest, we found that STAT1, a key transcriptional regulator in the Janus kinase (JAK)-STAT apoptotic pathway,[42] was much more abundant in ER-HCC tissue than in LR-HCC and surrounding liver tissues ($\Sigma_{emPAI} \approx 300$), and it was proteolyzed specifically in ER-HCC tissue (Figures 3A and 4A and Supplementary Table 6 in the Supporting Information).

dx.doi.org/10.1021/pr500262p | J. Proteome Res. XXXX, XXX, XXX–XXX

Table 2. Proteins Down-Regulated in the ER-HCC Tissue

UniProt ID	protein	molecular mass (kDa)	ΣemPAI minimum	degradation detected	oxido-reductase[a]	liver-specific expression[a,b]	phospho-protein[a]	previously reported HCC marker	ref
CPSM_HUMAN	carbamoyl-phosphate synthase	166256	0.0033	−	−	++	+	+	55−57
HPPD_HUPMN	4-hydroxyphenylpyruvate dioxygenase	45119	0.0048	−	+	−	+	−	
HBB_HUMAN	hemoglobin subunit beta	16130	0.0057	−	−	−	−	−	
DHB13_HUMAN	17-beta-hydroxysteroid dehydrogenase 13	34060	0.0087	−	+	++	−	−	
SARDH_HUMAN	sarcosine dehydrogenase, mitochondrial	102180	0.0088	−	+	−	−	−	
HBA_HUMAN	hemoglobin subunit alpha	15319	0.0099	−	−	−	−	+	58
APOB_HUMAN	apolipoprotein B-100	516988	0.0101	−	−	−	−	−	
ADO_HUMAN	aldehyde oxidase	150805	0.0115	+	+	++	−	+	59
PALM3_HUMAN	paralemmin-3	72078	0.0134	+	−	−	+	−	
GPDA_HUMAN	glycerol-3-phosphate dehydrogenase	38326	0.0142	−	+	−	−	−	
F16P1_HUMAN	fructose-1,6-bisphosphatase 1	37316	0.0176	−	−	−	−	+	60,61
AK1D1_HUMAN	3-oxo-5-beta-steroid 4-dehydrogenase	37779	0.0211	−	+	++	−	−	
CP3A4_HUMAN	cytochrome P450 3A4	57803	0.0219	−	+	++	−	−	
APOA_HUMAN	apolipoprotein(a)	518115	0.0224	+	−	−	−	−	
HUTU_HUMAN	urocanate hydratase	75777	0.0227	−	−	−	−	−	
ADH4_HUMAN	alcohol dehydrogenase 4	41332	0.0239	−	+	−	−	+	40
MY18A_HUMAN	myosin-XVIIIa	234463	0.0242	+	−	−	−	−	
UD14_HUMAN	UDP-glucuronosyltransferase 1−4	60767	0.0245	+	−	++	−	−	
REEP6_HUMAN	receptor expression-enhancing protein 6	20933	0.0253	−	−	−	−	−	
DOPD_HUMAN	D-dopachrome decarboxylase	12846	0.0255	−	−	−	−	−	
GYS2_HUMAN	glycogen [starch] synthase, liver	81719	0.0264	−	−	−	+	−	
UD16_HUMAN	UDP-glucuronosyltransferase 1−6	61493	0.0271	−	−	++	−	−	
ARK73_HUMAN	aflatoxin B1 aldehyde reductase member 3	37680	0.0278	−	+	+	−	−	
GUAD_HUMAN	guanine deaminase	51610	0.0289	−	−	−	−	−	
DHTK1_HUMAN	probable 2-oxoglutarate dehydrogenase E1 component DHKTD	103935	0.0317	−	+	−	−	−	
UD13_HUMAN	UDP-glucuronosyltransferase 1−3	61009	0.0345	+	−	−	−	−	
MTP_HUMAN	microsomal triglyceride transfer protein large subunit	100070	0.0352	+	−	++	−	−	
UD19_HUMAN	UDP-glucuronosyltransferase 1−9	60967	0.0359	+	−	++	−	−	
MYLK_HUMAN	myosin light chain kinase	213993	0.0365	+	−	±	+	−	
FMO5_HUMAN	dimethylanilme monooxygenase 5	60750	0.0371	+	+	++	−	−	
UD18_HUMAN	UDP-glucuronosyltransferase 1−8	60626	0.0375	+	−	−	−	−	
UD15_HUMAN	UDP-glucuronosyltransferase 1−5	60742	0.0377	+	−	−	−	−	
ADH6_HUMAN	alcohol dehydrogenase 6	40271	0.0379	+	+	++	−	−	
HBD_HUMAN	hemoglobin subunit delta	16187	0.0381	−	−	−	−	−	
AASS_HUMAN	alpha-aminoadipic semialdehyde synthase	102990	0.0417	−	+	++	−	−	
AL1L1_HUMAN	aldehyde dehydrogenase family 1 member L1	99832	0.0427	−	+	++	−	+	62
DDTL_HUMAN	D-dopachrome decarboxylase-like protein	14470	0.0429	−	−	−	−	−	
CRYM_HUMAN	mu-crystallin homologue	33967	0.0439	−	−	−	−	−	
UD17_HUMAN	UDP-glucuronosyltransferase 1−7	60774	0.0451	+	−	++	−	−	
CP3A7_HUMAN	cytochrome P450 3A7	57915	0.0487	−	+	−	−	−	
HAOX1_HUMAN	hydroxyacid oxidase 1	41183	0.0500	−	+	++	−	−	

[a]According to the UniProt database. [b]±, ubiquitous; +, moderately specific; ++, highly specific.

The corresponding peptographs indicated that the full-length STAT1, with an apparent molecular mass of 90 kDa, appeared to be cleaved into two major fragments in ER-HCC, a 38-kDa N-terminal fragment and a 45-kDa C-terminal fragment, whereas these cleavage fragments were barely detectible in the LR-HCC, AJ, and NL tissues (Figures 3A and 4A). STAT1 contains several structurally and functionally conserved domains, including a coiled-coil STAT domain implicated in protein−protein interactions, a DNA-binding domain with an immunoglobulin-like fold, an SH2 domain that acts as a phosphorylation-dependent switch to control cytokine receptor recognition and DNA-binding, and a C-terminal transactivation domain.[43] Interestingly, our peptograph analysis showed that the specific proteolysis of STAT1 occurred within the linker region between the DNA binding and SH2 domains (residues 321−359). This implies that deregulation of the JAK-STAT pathway may play a role in HCC recurrence by inducing aberrant transcription of genes associated with cell proliferation or programmed cell death.

dx.doi.org/10.1021/pr500262p | J. Proteome Res. XXXX, XXX, XXX−XXX

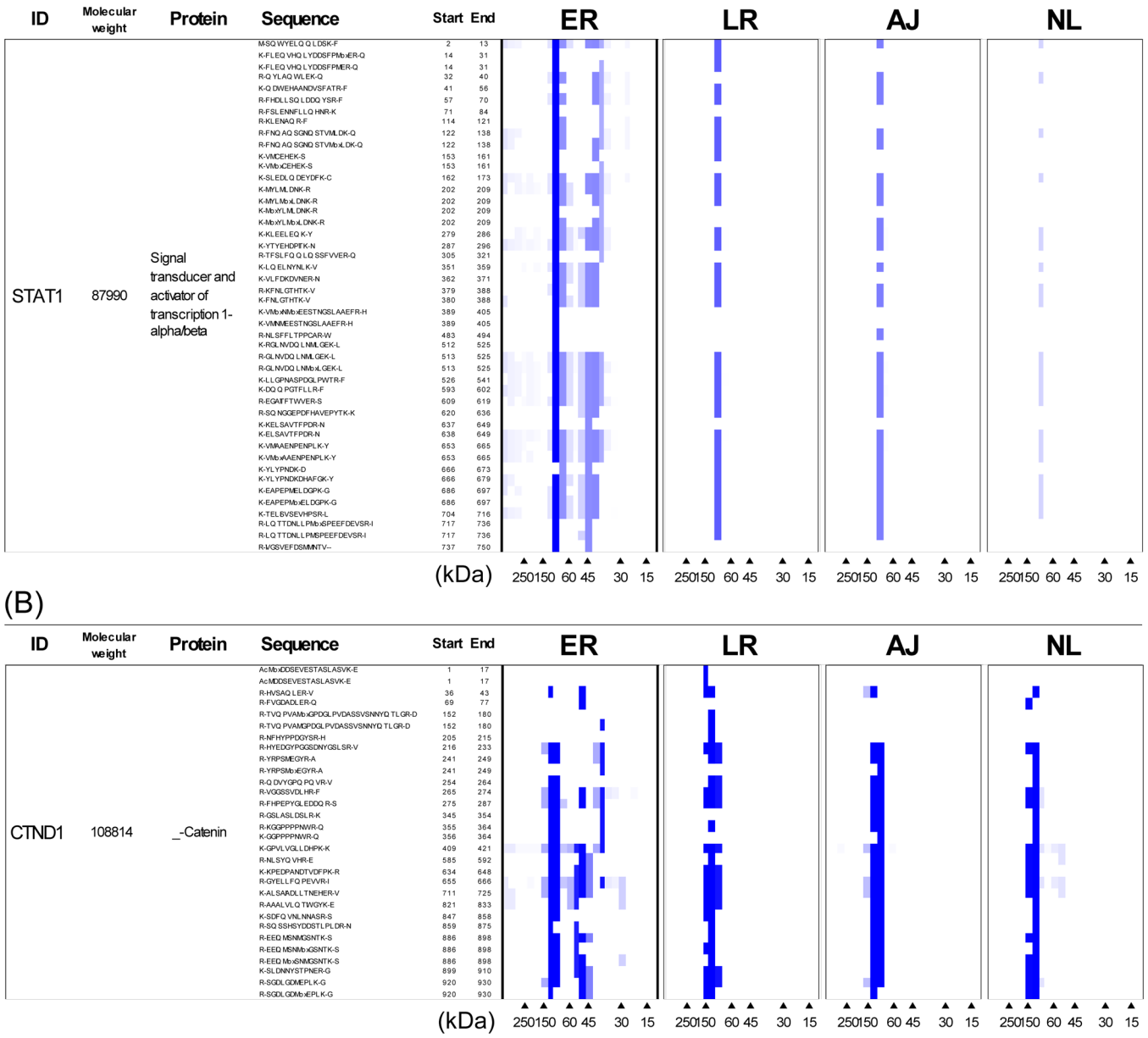

Figure 3. Proteolytic fragments of (A) STAT1 and (B) δ-catenin detected in the peptographs. Note that both STAT1 and δ-catenin have multiple ER-HCC tissue-specific proteolytic fragments.

The peptograph analysis also revealed that δ-catenin (110 kDa) underwent limited proteolysis to generate a number of fragments, including a 45 kDa N-terminal fragment and a 50 to 60 kDa C-terminal fragment (Figures 3B, 4B, and Supplementary Table 6 in the Supporting Information). This proteolysis was more prevalent in the ER-HCC tissue, as indicated by the peptograph ($\Sigma_{emPAI} \approx 40$) and by Western blot analysis (Figure 4B). δ-Catenin belongs to the β-catenin family and functions in the regulation of cell adhesion through the small GTPase pathway.[44] This protein is characterized by a coiled-coil domain (residues 10−46), 10 armadillo repeats (residues 358−826) that have a role in protein−protein interactions, and a nuclear localization signal at residues 622−634.[45] Interestingly, our peptograph analysis showed that the proteolysis of δ-catenin occurs between the third and fifth armadillo repeats (residues 385−584), a region that contains the C-, E-, and N-cadherin binding sites and thereby is critical for the maintenance of cell-surface stability.[46] This implies that aberrant δ-catenin proteolysis might destabilize cell adhesion, leading to metastasis of HCC cells. Thus, the PROTOMAP strategy provides new insight into the pathogenesis of HCC that will be explored in further investigations.

Proteolytic Fragments of STAT1 as a Key Indicator for Early Recurrence

To determine whether the proteolysis of STAT1 is a general characteristic of ER-HCC tissues, we examined multiple clinical specimens by Western blot analysis with the STAT1 antibody that detects the intact STAT1 molecule as well as its N- and C-terminal proteolytic fragments. Of the 10 individual clinical ER-HCC specimens examined, 4 contained the STAT1 proteolytic fragments (cases 16, 29, 31, and 39, Figure 5). Faint STAT1 fragments were also observed in the adjacent nontumor tissue

dx.doi.org/10.1021/pr500262p | J. Proteome Res. XXXX, XXX, XXX−XXX

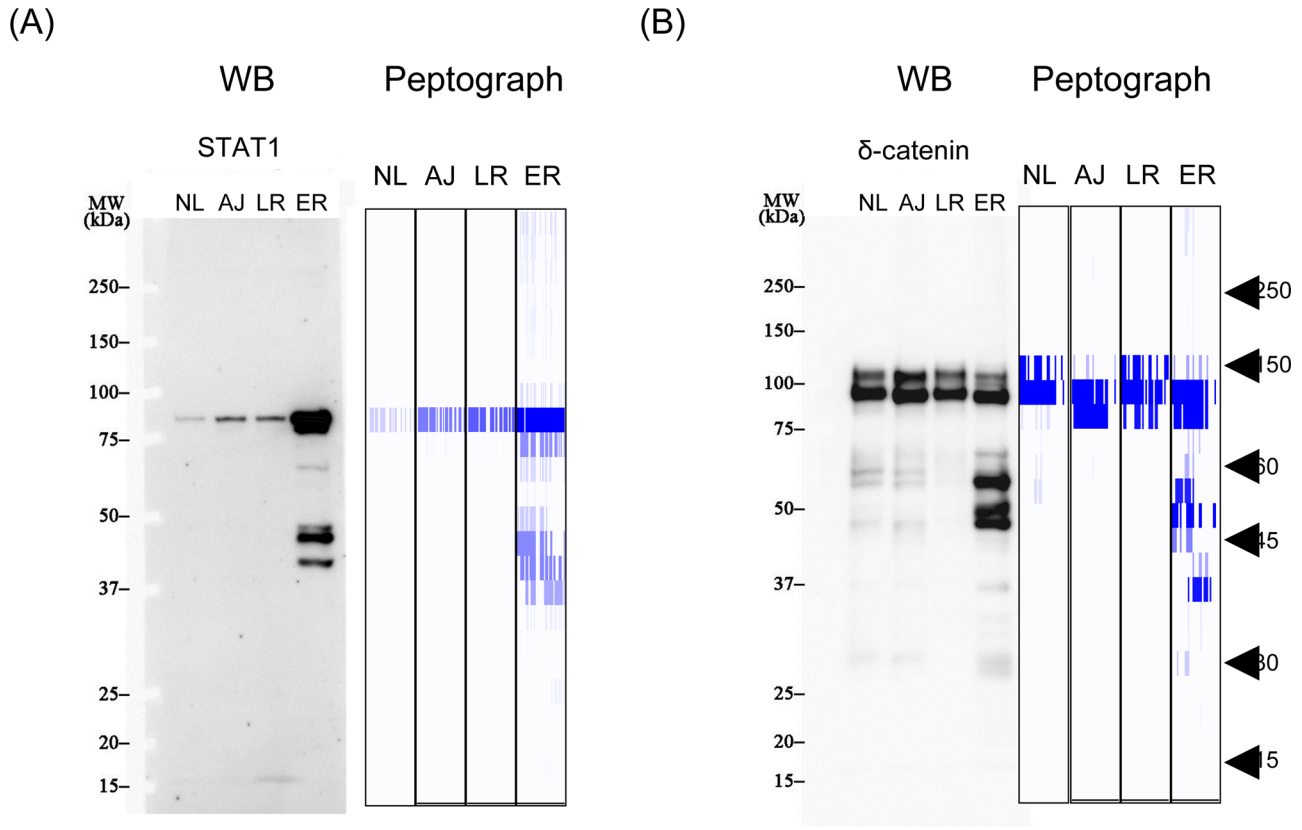

Figure 4. Western blot (WB) analysis and corresponding peptographs of (A) STAT1 and (B) δ-catenin in ER, LR, AJ, and NL tissues. The tissue used was the sample 18 (NL), 24 (AJ), 37 (LR), and 16 (ER) listed in Supplemental Table 1 in the Supporting Information, respectively. The peptographs are rotated 90° and their widths are reduced (relative Figure 3) to facilitate comparison.

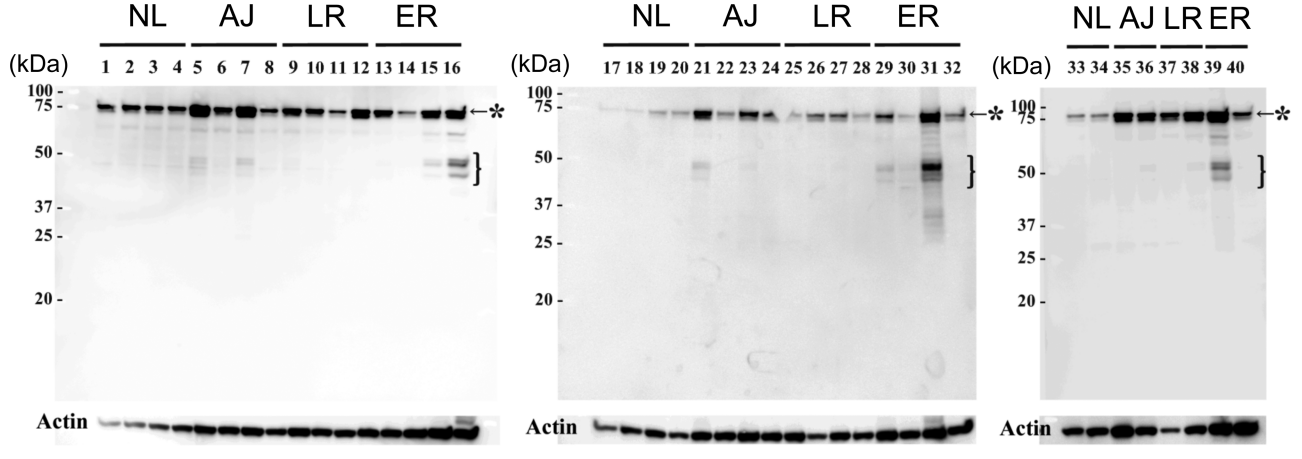

Figure 5. Western blot analysis of STAT1 in clinical tissue samples. The asterisk indicates the expected position of STAT1 according to the calculated molecular weight, and the bracket indicates the expected position of STAT1 peptide fragments according to MS. Note that the STAT1 peptide fragments were observed in a wide range of molecular weight using a gradient SDS-PAGE gel, and the main bands were observed at the expected molecular weight according to the PROTOMAP data. The sample information is given in Supplementary Table 1 in the Supporting Information. Actin was used as a loading control for the evaluation of protein quantities applied to the gel.

in three of these five ER-HCC cases (cases 5, 7 and 21, Figure 5). The STAT1 fragments were not observed in the 10 specimens from patients without recurrence within 2 years after surgery (i.e., patients with LR-HCC). These results suggest that ER-HCC tissues may be heterogeneous in terms of expression and proteolysis of STAT1. This is the first report of a potential functional role of STAT1 proteolysis in the recurrence of cancer, and further investigation of this role will expand our understanding of the biology of HCC. Moreover, these STAT1 proteolysis fragments may serve as a prognostic biomarker and may also lead to novel therapeutic strategies.

CONCLUSIONS

Here we have presented the first large-scale PROTOMAP profiling of HCC and surrounding liver tissues, which was aimed at the discovery of biomarker candidates for early prediction of the likelihood of recurrence. This analysis identified ~8500 unique proteins and a subset of ~87

dx.doi.org/10.1021/pr500262p | J. Proteome Res. XXXX, XXX, XXX−XXX

biomarker candidates with significantly altered levels in ER-HCC tissues. This protein subset contains many previously identified tumor biomarker candidates (Tables 1 and 2) and proteins with characteristic functional features; specifically, many of the up-regulated proteins are phosphoproteins with roles in signal transduction pathways, and many of the down-regulated proteins are involved in liver function pathways such as the urea cycle and detoxification metabolism. The most notable result of this study may be that proteolytic events appear to occur more frequently during tumorigenesis or recurrence of HCC than during normal liver proliferation. In particular, STAT1, a key transcriptional regulator of the JAK-STAT apoptotic signal transduction pathway, was proteolyzed specifically near the middle of the molecule in ER-HCC tissues, suggesting that the resulting STAT1 fragments may have pathological relevance and diagnostic potential for HCC. Likewise, we note that the aberrant proteolysis of δ-catenin may also have a role in HCC recurrence. Determination of the precise immunohistochemical localization of identified proteins using a proteome-wide antibody library such as Human Protein Atlas will be one of the intriguing challenges of our study. Finally, this study suggests that the PROTOMAP strategy will be useful in investigating the pathogenesis of ER-HCC and in identifying key potential biomarkers. The data set presented in this study will also likely serve as a useful resource for future HCC proteomics.

■ ASSOCIATED CONTENT

Supporting Information

Supplementary Figure 1: The molecular weight (A), subcellular distribution (B), and functional role (C) of proteins identified in this study. Supplementary Table 1: Clinicopathological features of donors. Supplementary Table 2: The peptides identified from ER by the PROTOMAP analysis. Supplementary Table 3: The peptides identified from LR by the PROTOMAP analysis. Supplementary Table 4: The peptides identified from AJ by the PROTOMAP analysis. Supplementary Table 5: The peptides identified from NL by the PROTOMAP analysis. Supplementary Table 6: Peptographs of HCC and related liver tissues. This material is available free of charge via the Internet at http://pubs.acs.org.

■ AUTHOR INFORMATION

Corresponding Authors

*T.I.: Tel: +81 426 77 5667. Fax: +81 426 77 2525. E-mail: isobe-toshiaki@tmu.ac.jp.
*T.K.: Tel: +81 3 3542 2511 (ext. 3004). Fax +81 3 3547 5298. E-mail: takondo@ncc.go.jp.

Present Addresses

▽N.M.: Department of Surgery, Kumiai Kosei Hospital, 1-1 Nakagiri-machi, Takayama-shi, Gifu 506-8502, Japan.
○H.O.: Department of Pathology, School of Medicine, Keio University, 35 Shinanomachi, Shinjuku-ku, Tokyo 160-0016, Japan.

Notes

The authors declare no competing financial interest.

■ ACKNOWLEDGMENTS

This work was supported by a grant for Advanced Scientific Research from the Tokyo Metropolitan Government.

■ ABBREVIATIONS:

ADH4, alcohol dehydrogenase 4; DAVID, Database for Annotation, Visualization and Integrated Discovery; emPAI, exponentially modified protein abundance index; ER, early recurrent; LR, late recurrent; AJ, nontumor tissue adjacent to the tumor; NL, normal liver tissue; HCC, hepatocellular carcinoma; JAK, Janus kinase; LC, liquid chromatography; MS, mass spectrometry; MS/MS, tandem mass spectrometry; PAGE, polyacrylamide gel electrophoresis; PROTOMAP, Protein Topography and Migration Analysis Platform; SDS, sodium dodecyl sulfate; STAT, Signal Transducers and Activators of Transcription family protein

■ REFERENCES

(1) Bosch, F. X.; Ribes, J.; Borras, J. Epidemiology of primary liver cancer. *Semin. Liver Dis.* **1999**, *19* (3), 271−285.
(2) Bruix, J.; Llovet, J. M. Major achievements in hepatocellular carcinoma. *Lancet* **2009**, *373* (9664), 614−616.
(3) Dudek, K.; Kornasiewicz, O.; Remiszewski, P.; Kobryn, K.; Ziarkiewicz-Wroblewska, B.; Gornicka, B.; Zieniewicz, K.; Krawczyk, M. Impact of tumor characteristic on the outcome of liver transplantation in patients with hepatocellular carcinoma. *Transplant. Proc.* **2009**, *41* (8), 3135−3137.
(4) Lim, K. C.; Chow, P. K.; Allen, J. C.; Chia, G. S.; Lim, M.; Cheow, P. C.; Chung, A. Y.; Ooi, L. L.; Tan, S. B. Microvascular invasion is a better predictor of tumor recurrence and overall survival following surgical resection for hepatocellular carcinoma compared to the Milan criteria. *Ann. Surg.* **2011**, *254* (1), 108−113.
(5) Mazzaferro, V.; Llovet, J. M.; Miceli, R.; Bhoori, S.; Schiavo, M.; Mariani, L.; Camerini, T.; Roayaie, S.; Schwartz, M. E.; Grazi, G. L.; Adam, R.; Neuhaus, P.; Salizzoni, M.; Bruix, J.; Forner, A.; De Carlis, L.; Cillo, U.; Burroughs, A. K.; Troisi, R.; Rossi, M.; Gerunda, G. E.; Lerut, J.; Belghiti, J.; Boin, I.; Gugenheim, J.; Rochling, F.; Van Hoek, B.; Majno, P. Predicting survival after liver transplantation in patients with hepatocellular carcinoma beyond the Milan criteria: a retrospective, exploratory analysis. *Lancet Oncol.* **2009**, *10* (1), 35−43.
(6) Poon, R. T. Differentiating early and late recurrences after resection of HCC in cirrhotic patients: implications on surveillance, prevention, and treatment strategies. *Ann. Surg. Oncol.* **2009**, *16* (4), 792−794.
(7) Roayaie, S.; Blume, I. N.; Thung, S. N.; Guido, M.; Fiel, M. I.; Hiotis, S.; Labow, D. M.; Llovet, J. M.; Schwartz, M. E. A system of classifying microvascular invasion to predict outcome after resection in patients with hepatocellular carcinoma. *Gastroenterology* **2009**, *137* (3), 850−855.
(8) Llovet, J. M.; Bruix, J. Novel advancements in the management of hepatocellular carcinoma in 2008. *J. Hepatol.* **2008**, *48* (Suppl 1), S20−S37.
(9) Iizuka, N.; Oka, M.; Yamada-Okabe, H.; Nishida, M.; Maeda, Y.; Mori, N.; Takao, T.; Tamesa, T.; Tangoku, A.; Tabuchi, H.; Hamada, K.; Nakayama, H.; Ishitsuka, H.; Miyamoto, T.; Hirabayashi, A.; Uchimura, S.; Hamamoto, Y. Oligonucleotide microarray for prediction of early intrahepatic recurrence of hepatocellular carcinoma after curative resection. *Lancet* **2003**, *361* (9361), 923−929.
(10) Ye, Q. H.; Qin, L. X.; Forgues, M.; He, P.; Kim, J. W.; Peng, A. C.; Simon, R.; Li, Y.; Robles, A. I.; Chen, Y.; Ma, Z. C.; Wu, Z. Q.; Ye, S. L.; Liu, Y. K.; Tang, Z. Y.; Wang, X. W. Predicting hepatitis B virus-positive metastatic hepatocellular carcinomas using gene expression profiling and supervised machine learning. *Nat. Med.* **2003**, *9* (4), 416−423.
(11) Du, Y.; Cao, G. W. Challenges of incorporating gene expression data to predict HCC prognosis in the age of systems biology. *World J. Gastroenterol* **2012**, *18* (30), 3941−3944.
(12) Orimo, T.; Ojima, H.; Hiraoka, N.; Saito, S.; Kosuge, T.; Kakisaka, T.; Yokoo, H.; Nakanishi, K.; Kamiyama, T.; Todo, S.; Hirohashi, S.; Kondo, T. Proteomic profiling reveals the prognostic

value of adenomatous polyposis coli-end-binding protein 1 in hepatocellular carcinoma. *Hepatology* **2008**, *48* (6), 1851−1863.
(13) Bai, D. S.; Dai, Z.; Zhou, J.; Liu, Y. K.; Qiu, S. J.; Tan, C. J.; Shi, Y. H.; Huang, C.; Wang, Z.; He, Y. F.; Fan, J. Capn4 overexpression underlies tumor invasion and metastasis after liver transplantation for hepatocellular carcinoma. *Hepatology* **2009**, *49* (2), 460−470.
(14) Yi, X.; Luk, J. M.; Lee, N. P.; Peng, J.; Leng, X.; Guan, X. Y.; Lau, G. K.; Beretta, L.; Fan, S. T. Association of mortalin (HSPA9) with liver cancer metastasis and prediction for early tumor recurrence. *Mol. Cell. Proteomics* **2008**, *7* (2), 315−325.
(15) Kanamori, H.; Kawakami, T.; Effendi, K.; Yamazaki, K.; Mori, T.; Ebinuma, H.; Masugi, Y.; Du, W.; Nagasaka, K.; Ogiwara, A.; Kyono, Y.; Tanabe, M.; Saito, H.; Hibi, T.; Sakamoto, M. Identification by differential tissue proteome analysis of talin-1 as a novel molecular marker of progression of hepatocellular carcinoma. *Oncology* **2011**, *80* (5−6), 406−415.
(16) Lee, S. H.; Shin, M. S.; Lee, H. S.; Bae, J. H.; Lee, H. K.; Kim, H. S.; Kim, S. Y.; Jang, J. J.; Joo, M.; Kang, Y. K.; Park, W. S.; Park, J. Y.; Oh, R. R.; Han, S. Y.; Lee, J. H.; Kim, S. H.; Lee, J. Y.; Yoo, N. J. Expression of Fas and Fas-related molecules in human hepatocellular carcinoma. *Hum. Pathol.* **2001**, *32* (3), 250−256.
(17) Volkmann, M.; Schiff, J. H.; Hajjar, Y.; Otto, G.; Stilgenbauer, F.; Fiehn, W.; Galle, P. R.; Hofmann, W. J. Loss of CD95 expression is linked to most but not all p53 mutants in European hepatocellular carcinoma. *J. Mol. Med. (Heidelberg, Ger.)* **2001**, *79* (10), 594−600.
(18) Marquardt, J. U.; Galle, P. R.; Teufel, A. Molecular diagnosis and therapy of hepatocellular carcinoma (HCC): an emerging field for advanced technologies. *J. Hepatol.* **2012**, *56* (1), 267−275.
(19) Turgeon, V. L.; Houenou, L. J. The role of thrombin-like (serine) proteases in the development, plasticity and pathology of the nervous system. *Brain Res. Rev.* **1997**, *25* (1), 85−95.
(20) Riewald, M.; Ruf, W. Mechanistic coupling of protease signaling and initiation of coagulation by tissue factor. *Proc. Natl. Acad. Sci. U. S. A.* **2001**, *98* (14), 7742−7747.
(21) Alnemri, E. S. Mammalian cell death proteases: a family of highly conserved aspartate specific cysteine proteases. *J. Cell Biochem.* **1997**, *64* (1), 33−42.
(22) Abdel-Rahman, H. M.; Kimura, T.; Hidaka, K.; Kiso, A.; Nezami, A.; Freire, E.; Hayashi, Y.; Kiso, Y. Design of inhibitors against HIV, HTLV-I, and Plasmodium falciparum aspartic proteases. *Biol. Chem.* **2004**, *385* (11), 1035−1039.
(23) van Kempen, L. C.; de Visser, K. E.; Coussens, L. M. Inflammation, proteases and cancer. *Eur. J. Cancer* **2006**, *42* (6), 728−734.
(24) Quesada, V.; Ordonez, G. R.; Sanchez, L. M.; Puente, X. S.; Lopez-Otin, C. The Degradome database: mammalian proteases and diseases of proteolysis. *Nucleic Acids Res.* **2009**, *37* (Database issue), D239−D243.
(25) Nisman, B.; Biran, H.; Heching, N.; Barak, V.; Ramu, N.; Nemirovsky, I.; Peretz, T. Prognostic role of serum cytokeratin 19 fragments in advanced non-small-cell lung cancer: association of marker changes after two chemotherapy cycles with different measures of clinical response and survival. *Br. J. Cancer* **2008**, *98* (1), 77−79.
(26) Streckfus, C.; Bigler, L.; Tucci, M.; Thigpen, J. T. A preliminary study of CA15−3, c-erbB-2, epidermal growth factor receptor, cathepsin-D, and p53 in saliva among women with breast carcinoma. *Cancer Invest.* **2000**, *18* (2), 101−109.
(27) Dix, M. M.; Simon, G. M.; Cravatt, B. F. Global mapping of the topography and magnitude of proteolytic events in apoptosis. *Cell* **2008**, *134* (4), 679−691.
(28) Shen, C.; Yu, Y.; Li, H.; Yan, G.; Liu, M.; Shen, H.; Yang, P. Global profiling of proteolytically modified proteins in human metastatic hepatocellular carcinoma cell lines reveals CAPN2 centered network. *Proteomics* **2012**, *12* (12), 1917−1927.
(29) Ishihama, Y.; Oda, Y.; Tabata, T.; Sato, T.; Nagasu, T.; Rappsilber, J.; Mann, M. Exponentially modified protein abundance index (emPAI) for estimation of absolute protein amount in proteomics by the number of sequenced peptides per protein. *Mol. Cell. Proteomics* **2005**, *4* (9), 1265−1272.
(30) Taoka, M.; Wakamiya, A.; Nakayama, H.; Isobe, T. Protein profiling of rat cerebella during development. *Electrophoresis* **2000**, *21* (9), 1872−1879.
(31) Abiko, M.; Furuta, K.; Yamauchi, Y.; Fujita, C.; Taoka, M.; Isobe, T.; Okamoto, T. Identification of proteins enriched in rice egg or sperm cells by single-cell proteomics. *PLoS One* **2013**, *8* (7), e69578.
(32) Taoka, M.; Yamauchi, Y.; Nobe, Y.; Masaki, S.; Nakayama, H.; Ishikawa, H.; Takahashi, N.; Isobe, T. An analytical platform for mass spectrometry-based identification and chemical analysis of RNA in ribonucleoprotein complexes. *Nucleic Acids Res.* **2009**, *37* (21), e140.
(33) Shinkawa, T.; Taoka, M.; Yamauchi, Y.; Ichimura, T.; Kaji, H.; Takahashi, N.; Isobe, T. STEM: a software tool for large-scale proteomic data analyses. *J. Proteome Res.* **2005**, *4* (5), 1826−1831.
(34) Corrocher, R.; Casaril, M.; Bellisola, G.; Gabrielli, G. B.; Nicoli, N.; Guidi, G. C.; De Sandre, G. Severe impairment of antioxidant system in human hepatoma. *Cancer* **1986**, *58* (8), 1658−1662.
(35) Sato, K.; Ito, K.; Kohara, H.; Yamaguchi, Y.; Adachi, K.; Endo, H. Negative regulation of catalase gene expression in hepatoma cells. *Mol. Cell. Biol.* **1992**, *12* (6), 2525−2533.
(36) Sun, Y.; Oberley, L. W.; Oberley, T. D.; Elwell, J. H.; Sierra-Rivera, E. Lowered antioxidant enzymes in spontaneously transformed embryonic mouse liver cells in culture. *Carcinogenesis* **1993**, *14* (7), 1457−1463.
(37) Qiu, W.; David, D.; Zhou, B.; Chu, P. G.; Zhang, B.; Wu, M.; Xiao, J.; Han, T.; Zhu, Z.; Wang, T.; Liu, X.; Lopez, R.; Frankel, P.; Jong, A.; Yen, Y. Down-regulation of growth arrest DNA damage-inducible gene 45beta expression is associated with human hepatocellular carcinoma. *Am. J. Pathol.* **2003**, *162* (6), 1961−1974.
(38) Ho, J. C.; Cheung, S. T.; Leung, K. L.; Ng, I. O.; Fan, S. T. Decreased expression of cytochrome P450 2E1 is associated with poor prognosis of hepatocellular carcinoma. *Int. J. Cancer* **2004**, *111* (4), 494−500.
(39) Ngoka, L. C. Dramatic down-regulation of oxidoreductases in human hepatocellular carcinoma hepG2 cells: proteomics and gene ontology unveiling new frontiers in cancer enzymology. *Proteome Sci.* **2008**, *6*, 29.
(40) Wei, R. R.; Zhang, M. Y.; Rao, H. L.; Pu, H. Y.; Zhang, H. Z.; Wang, H. Y. Identification of ADH4 as a novel and potential prognostic marker in hepatocellular carcinoma. *Med. Oncol* **2012**, *29* (4), 2737−2743.
(41) Jordan, C. T.; Guzman, M. L.; Noble, M. Cancer stem cells. *N. Engl J. Med.* **2006**, *355* (12), 1253−1261.
(42) Stark, G. R.; Darnell, J. E., Jr. The JAK-STAT pathway at twenty. *Immunity* **2012**, *36* (4), 503−514.
(43) Chen, X.; Vinkemeier, U.; Zhao, Y.; Jeruzalmi, D.; Darnell, J. E., Jr.; Kuriyan, J. Crystal structure of a tyrosine phosphorylated STAT-1 dimer bound to DNA. *Cell* **1998**, *93* (5), 827−839.
(44) Menke, A.; Giehl, K. Regulation of adherens junctions by Rho GTPases and p120-catenin. *Arch. Biochem. Biophys.* **2012**, *524* (1), 48−55.
(45) McCrea, P. D.; Park, J. I. Developmental functions of the P120-catenin sub-family. *Biochim. Biophys. Acta* **2007**, *1773* (1), 17−33.
(46) Ishiyama, N.; Lee, S. H.; Liu, S.; Li, G. Y.; Smith, M. J.; Reichardt, L. F.; Ikura, M. Dynamic and static interactions between p120 catenin and E-cadherin regulate the stability of cell-cell adhesion. *Cell* **2010**, *141* (1), 117−128.
(47) Torbenson, M.; Wang, J.; Choti, M.; Ashfaq, R.; Maitra, A.; Wilentz, R. E.; Boitnott, J. Hepatocellular carcinomas show abnormal expression of fibronectin protein. *Mod. Pathol.* **2002**, *15* (8), 826−830.
(48) Matsui, S.; Takahashi, T.; Oyanagi, Y.; Takahashi, S.; Boku, S.; Takahashi, K.; Furukawa, K.; Arai, F.; Asakura, H. Expression, localization and alternative splicing pattern of fibronectin messenger RNA in fibrotic human liver and hepatocellular carcinoma. *J. Hepatol.* **1997**, *27* (5), 843−853.
(49) Haglund, C.; Ylatupa, S.; Mertaniemi, P.; Partanen, P. Cellular fibronectin concentration in the plasma of patients with malignant and benign diseases: a comparison with CA 19−9 and CEA. *Br. J. Cancer* **1997**, *76* (6), 777−783.

(50) Chen, X. L.; Zhou, L.; Yang, J.; Shen, F. K.; Zhao, S. P.; Wang, Y. L. Hepatocellular carcinoma-associated protein markers investigated by MALDI-TOF MS. *Mol. Med. Rep.* **2011**, *3* (4), 589−596.
(51) Luk, J. M.; Lam, C. T.; Siu, A. F.; Lam, B. Y.; Ng, I. O.; Hu, M. Y.; Che, C. M.; Fan, S. T. Proteomic profiling of hepatocellular carcinoma in Chinese cohort reveals heat-shock proteins (Hsp27, Hsp70, GRP78) up-regulation and their associated prognostic values. *Proteomics* **2006**, *6* (3), 1049−1057.
(52) Song, H. Y.; Liu, Y. K.; Feng, J. T.; Cui, J. F.; Dai, Z.; Zhang, L. J.; Feng, J. X.; Shen, H. L.; Tang, Z. Y. Proteomic analysis on metastasis-associated proteins of human hepatocellular carcinoma tissues. *J. Cancer Res. Clin. Oncol.* **2006**, *132* (2), 92−98.
(53) Yokota, S.; Yamamoto, Y.; Shimizu, K.; Momoi, H.; Kamikawa, T.; Yamaoka, Y.; Yanagi, H.; Yura, T.; Kubota, H. Increased expression of cytosolic chaperonin CCT in human hepatocellular and colonic carcinoma. *Cell Stress Chaperones* **2001**, *6* (4), 345−350.
(54) Sung, Y. K.; Hwang, S. Y.; Park, M. K.; Bae, H. I.; Kim, W. H.; Kim, J. C.; Kim, M. Fatty acid-CoA ligase 4 is overexpressed in human hepatocellular carcinoma. *Cancer Sci.* **2003**, *94* (5), 421−424.
(55) Liu, H.; Dong, H.; Robertson, K.; Liu, C. DNA methylation suppresses expression of the urea cycle enzyme carbamoyl phosphate synthetase 1 (CPS1) in human hepatocellular carcinoma. *Am. J. Pathol.* **2011**, *178* (2), 652−661.
(56) Cardona, D. M.; Zhang, X.; Liu, C. Loss of carbamoyl phosphate synthetase I in small-intestinal adenocarcinoma. *Am. J. Clin. Pathol.* **2009**, *132* (6), 877−882.
(57) Butler, S. L.; Dong, H.; Cardona, D.; Jia, M.; Zheng, R.; Zhu, H.; Crawford, J. M.; Liu, C. The antigen for Hep Par 1 antibody is the urea cycle enzyme carbamoyl phosphate synthetase 1. *Lab. Invest.* **2008**, *88* (1), 78−88.
(58) Matos, J. M.; Witzmann, F. A.; Cummings, O. W.; Schmidt, C. M. A pilot study of proteomic profiles of human hepatocellular carcinoma in the United States. *J. Surg. Res.* **2009**, *155* (2), 237−243.
(59) Sigruener, A.; Buechler, C.; Orso, E.; Hartmann, A.; Wild, P. J.; Terracciano, L.; Roncalli, M.; Bornstein, S. R.; Schmitz, G. Human aldehyde oxidase 1 interacts with ATP-binding cassette transporter-1 and modulates its activity in hepatocytes. *Horm. Metab. Res.* **2007**, *39* (11), 781−789.
(60) Chen, M.; Zhang, J.; Li, N.; Qian, Z.; Zhu, M.; Li, Q.; Zheng, J.; Wang, X.; Shi, G. Promoter hypermethylation mediated down-regulation of FBP1 in human hepatocellular carcinoma and colon cancer. *PLoS One* **2011**, *6* (10), e25564.
(61) Liu, Z.; Ma, Y.; Yang, J.; Qin, H. Upregulated and downregulated proteins in hepatocellular carcinoma: a systematic review of proteomic profiling studies. *OMICS* **2011**, *15* (1−2), 61−71.
(62) Chen, X. Q.; He, J. R.; Wang, H. Y. Decreased expression of ALDH1L1 is associated with a poor prognosis in hepatocellular carcinoma. *Med. Oncol.* **2012**, *29* (3), 1843−1849.